TIME-DEPENDENT METHOD FOR MANY-BODY PROBLEMS AND ITS APPLICATION TO NUCLEAR RESONANT SYSTEMS*

Tomohiro Oishi[†], Lorenzo Fortunato

Department of Physics and Astronomy "Galileo Galilei", University of Padova
Via Marzolo 8, 35131 Padova, Italy
and
INFN — Sezione di Padova, Via Marzolo 8, 35131 Padova, Italy

The decay process of the schematic one-dimensional three-body system is considered. A time-dependent approach is used in combination with a one-dimensional three-body model, which is composed of a heavier core nucleus and two nucleons, with the aim of describing its evolution in two-nucleon emission. The process is calculated from the initial state, in which the three ingredient particles are confined. In this process, two different types of emission can be found: the earlier process includes the emission of spatially correlated two-nucleon pair, like a dinucleon, whereas, at a subsequent time, all the particles are separated from each other. The time-dependent method can be a suitable option to investigate the meta-stable and/or open-quantum systems, where the complicated many-body dynamics should necessarily be taken into account.

1. Introduction

Quantum resonance or meta-stability is a basic concept to understand several dynamical processes in atomic nuclei. Those include, *e.g.* two-proton or two-neutron emission [1–3], tetra neutron [4, 5], and alpha-clustering resonant states (*c.f.* Hoyle state of ^{12}C) [6–9]. By investigating these processes, we expect to obtain fundamental information on nuclear interaction, multi-spin dynamics, and/or quantum tunneling effect in systems with many degrees of freedom.

---

* Presented at the XXXV Mazurian Lakes Conference on Physics, Piaski, Poland, September 3–9, 2017.

† Corresponding author: `toishi@pd.infn.it`

On the theoretical side, however, the description of these meta-stable systems has been a long-standing problem. The usual quantum mechanics for bound states should be extended to dealing with the meta-stability and the multi-particle degrees of freedom on equal footing [1, 8, 10]. For this purpose, we have developed a time-dependent three-body model for theoretical and computational approach [11–14]. This method can provide an intuitive way to discuss even the broad-resonance system, whose lifetime is considerably short, and thus the multi-particle dynamics should be taken into account.

In this work, we perform a toy-model calculation to investigate the broad-resonance state. We utilize the time-dependent method to describe the scattering emission from the three-body localization. In contrast to the radioactive processes, it is not guaranteed that this emission process can be attributed to a single quasi-stationary state, but we to take into account the contribution from all the possible components.

In the next section, we employ one-dimensional three-body model as our testing field for time-dependent calculation. Section 3 is devoted to present our results and discussions. Finally, we summarize this article in Section 4.

2. Model and formalism

In this work, we give an example of the time-dependent (TD) calculation, implemented into a three-body system in one dimension (1D) [15]. The total Hamiltonian is

$$H_{\text{tot}} = \sum_{i=1}^{3} \frac{p_i^2}{2m_i} + V_{12}(|x_1 - x_2|) + V_{23}(|x_2 - x_3|) + V_{13}(|x_1 - x_3|). \quad (1)$$

We employ the masses of particles defined as $m_1 = m_2 = 939$ MeV/c^2 and $m_3 = 16 \times 939$ MeV/c^2. Namely, we assume a heavy-core nucleus and two nucleons moving on the one-dimensional x-axis (see Fig. 1), mimicking the ^{18}O nucleus but without pretending a realistic description. For the nucleon–nucleon subsystem, we employ a square-well attractive potential. That is,

$$V_{12}(x) = \begin{cases} -2.84 \text{ MeV} & (|x| \le 1.2 \text{ fm}), \\ 0 & (|x| > 1.2 \text{ fm}). \end{cases} \quad (2)$$

For the core–nucleon channel, on the other hand,

$$V_{13}(x) = V_{23}(x) = V_r \exp\left(-\frac{x^2}{d_r^2}\right) + V_a \exp\left(-\frac{x^2}{d_a^2}\right), \quad (3)$$

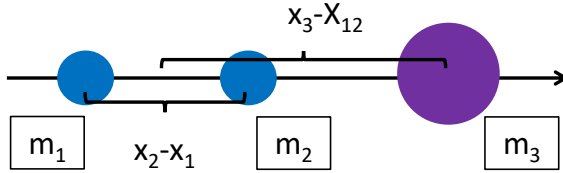where $d_r = 5.04$ fm, $d_a = 3.15$ fm, $V_r = 24$ MeV and $V_a = -32$ MeV.

Fig. 1. Three-body system in one dimension. $X_{12} = (x_1 + x_2)/2$.

These potentials are shown in Fig. 2. The bump in the core–nucleon potential can be associated with the centrifugal barrier in the realistic nuclei. Note that, in this work, we focus on the broad-resonance state. For this purpose, the two-body potentials are fixed shallower than the usual potentials in the three-dimensional calculations. Also, instead of the Woods–Saxon-type, we employ the Gaussian potential, which enables us to utilize the analytic formula to obtain the matrix elements with the harmonic oscillator (HO) basis employed in the next subsection.
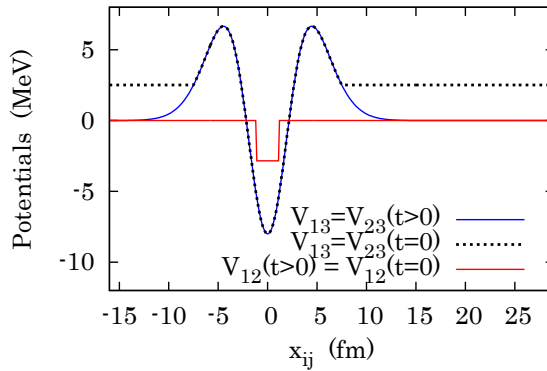

Fig. 2. Two-body potentials as functions of the relative distances, $x_{ij} \equiv (x_i - x_j)$.

2.1. Coordinates and basis

In order to solve the eigen-states of H_{3b}, we first employ the mass-scaled Jacobi coordinates (MSJC) [16, 17]. Using the common-relative mass, $\mu \equiv \sqrt{\prod_{i=1}^{3} m_i / \sum_{i=1}^{3} m_i}$, those are defined as

$$\xi_1 = \sqrt{\frac{\mu_1}{\mu}}(x_2 - x_1), \qquad \xi_2 = \sqrt{\frac{\mu_2}{\mu}}\left(x_3 - \frac{x_2 + x_1}{2}\right), \qquad (4)$$

and $\xi_3 \equiv (m_1 x_1 + m_2 x_2 + m_3 x_3)/\sum_{i=1}^{3} m_i$, which is the center-of-mass coordinate. Partial relative masses are defined as $\mu_k \equiv m_{k+1} \sum_{i=1}^{k} m_i / \sum_{j=1}^{k+1} m_j$,

for $k = 1$ and 2. With MSJC, the total Hamiltonian reads

$$H_{\text{tot}} = T_{\text{CM}} + \frac{\pi_1^2}{2\mu} + \frac{\pi_2^2}{2\mu} + V_{12} + V_{23} + V_{13},$$

$$T_{\text{CM}} = \frac{\pi_3^2}{2(m_1 + m_2 + m_3)}, \tag{5}$$

where $\{\pi_i\}$ are the conjugate momenta to $\{\xi_i\}$. In the following, we neglect the center-of-mass motion, T_{CM}. We diagonalize the remaining Hamiltonian, $H_{3b} = H_{\text{tot}} - T_{\text{CM}}$, by calculating its matrix elements, $\langle \Psi_{cd}|H_{3b}|\Psi_{ab}\rangle$, within the harmonic oscillator (HO) basis

$$\Psi_{ab}(\xi_1, \xi_2) = \psi_a(\xi_1)\psi_b(\xi_2), \tag{6}$$

where a and b are non-negative integers. Notice that ψ_n is the HO wave function corresponding either to the relative motion of particles 1 and 2, or the motion of particle 3 with respect to the center-of-mass between 1 and 2, with HO energy, $(n+1/2)\hbar\omega$. Our model space is truncated as $a, b \leq 15$ with $\hbar\omega = 0.4$ MeV. This value is chosen in a range that insures the convergence.

In this article, we assume that two nucleons have the spin-singlet configuration: $|S_{12} = 0\rangle = (|\uparrow\downarrow\rangle - |\downarrow\uparrow\rangle)/\sqrt{2}$. Thus, the spatial part should be symmetric against the exchange between particles 1 and 2. It means that only $\{\psi_a(\xi_1)\}$ with even a can be included in our basis.

Within the chosen MSJC scheme, the matrix elements of V_{12} are diagonal, whereas V_{23} and V_{13} yield non-diagonal components. For computation of these non-diagonal elements, we utilized a kinetic rotation technique, whose details can be found in Ref. [15]. Then, all the eigen-states, $H_{3b}|\Phi_M\rangle = E_M|\Phi_M\rangle$, can be solved by diagonalization: $|\Phi_M\rangle = \sum_{ab} c_{M,ab}|\Psi_{ab}\rangle$.

2.2. Initial state for time evolution

We employ the confining potential method for time-evolution. This method has provided a good approximation for quantum meta-stable phenomena especially in nuclear physics [11–13]. For the confining potential, $V_{13}^{(c)} = V_{23}^{(c)}$ at $t = 0$ fm/c, we fix the wall potential from $|x_i - x_j| \geq 7.5$ fm. On the other hand, V_{12} between the light two particles is unchanged. See Fig. 2 for visual plots of these potentials. Our initial state, $|\Upsilon(t = 0)\rangle$, is solved by diagonalizing the confining Hamiltonian including $V_{13}^{(c)}$ and $V_{23}^{(c)}$. It is also worthwhile to note that the initial state can be expanded on the eigen-states of the true Hamiltonian

$$|\Upsilon(t = 0)\rangle = \sum_M d_M(0)|\Phi_M\rangle. \tag{7}$$

For this initial state, after the subtraction of the center-of-mass motion, the expectation value of the relative Hamiltonian is given as $\langle \Upsilon(0)|H_{3b}|\Upsilon(0)\rangle = 0.91$ MeV. This is equivalent to the energy release (Q-value) carried out by the emitted particles.

3. Result and discussion

In the first panel of Fig. 3, we plot the density distribution of the initial state: $\rho(t = 0) = |\Upsilon(t = 0; \xi_1, \xi_2)|^2$. As expected, the three ingredient particles are spatially localized at $t = 0$.
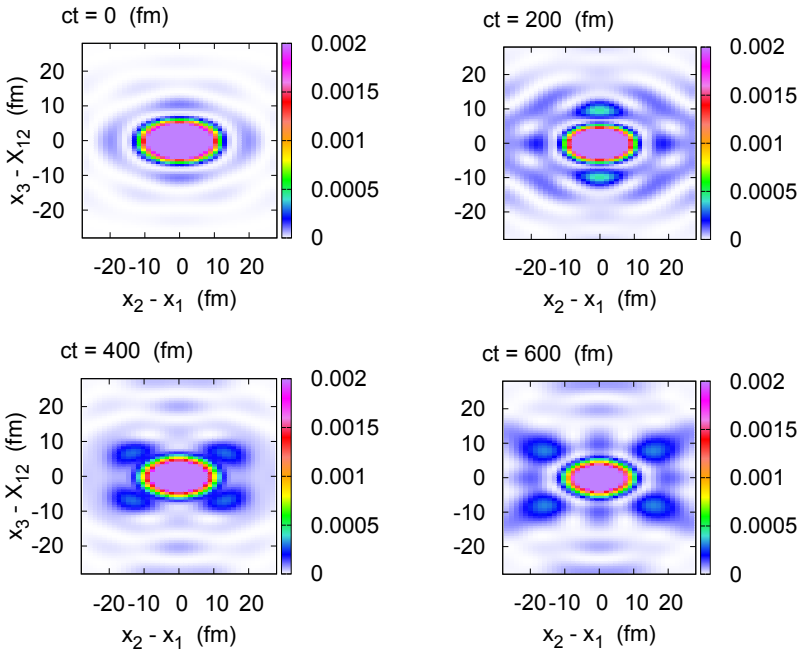

Fig. 3. Density distribution, $\rho(t) = |\Upsilon(t)|^2$, for $ct = 0, 200, 400$ and 600 fm. These are plotted as functions of $x_1 - x_2$ and $x_3 - X_{12}$, where X_{12} is the center-of-mass between the 1st and 2nd particles.

3.1. Time-dependent emission

From Eq. (7), time-evolution via H_{3b} can be calculated as

$$|\Upsilon(t)\rangle \equiv \exp\left[-it\frac{H_{3b}}{\hbar}\right]|\Upsilon(t = 0)\rangle = \sum_M d_M(t)|\Phi_M\rangle, \qquad \text{where}$$

$$d_M(t) = e^{-itE_M/\hbar}d_M(0). \tag{8}$$

298 T. OISHI, L. FORTUNATO

The time-evolution of the density distribution is shown in Fig. 3. That is,

$$\rho(t; \xi_1, \xi_2) = |\Upsilon(t; \xi_1, \xi_2)|^2 . \tag{9}$$

Notice that the energy distribution is invariant during the time-evolution: $s(E_M) \equiv |d_M(0)|^2 = |d_M(t)|^2$. In Fig. 4, we plot the energy distribution. From this result, we can find that the state of interest, $|\Upsilon(t)\rangle$, can be mostly attributed to the low-lying components with continuum energies up to $E \leq$ 1.8 MeV.
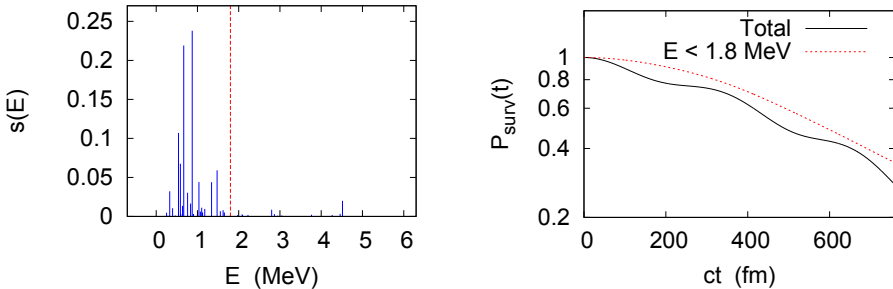

Fig. 4. (Left panel) Energy spectrum of the emission state, $|\Upsilon(t)\rangle$. $E_T = 1.8$ MeV is indicated by the dashed line. (Right panel) Survival probability.

In Fig. 3, at $ct = 200$ fm, the emission process proceeds mainly with $x_2 = x_1$ and $x_3 - X_{12} = \pm 10$ fm, where X_{12} indicates $(x_1 + x_2)/2$. This earlier process means that the two light particles, m_1 and m_2, are spatially correlated and emitted as a pair from the core. Namely, we observe a dinucleon emission in 1D space [13].

After $ct \geq 400$ fm as shown in Fig. 3, on the other hand, the process shows a different pattern with $|x_2 - x_1| \simeq 15$ fm and $|x_3 - X_{12}| \simeq 10$ fm. In this process, the two light particles are not localized anymore, and three particles move away from each other. Thus, the total emission should be a superposition of the primary dinucleon emission and the secondary separated emission. This superposition is quite in contrast to Ref. [13], where only the dinucleon emission is dominant with the pairing force. In such a way, our time-dependent method can provide a direct and intuitive solution to describe this complex quantum dynamics.

3.2. Survival probability

First, we define the decay state, $|\Upsilon_d(t)\rangle$, such as

$$|\Upsilon_d(t)\rangle \equiv |\Upsilon(t)\rangle - \beta(t)|\Upsilon(0)\rangle = \sum_M y_M(t)|\Phi_M\rangle , \tag{10}$$

where $\beta(t) \equiv \langle \Upsilon(0)|\Upsilon(t)\rangle$ and $y_M(t) = d_M(t) - \beta(t)d_M(0)$. Notice that $\langle \Upsilon(0)|\Upsilon_d(t)\rangle = 0$. Also, the decay probability can be formulated as $P_{\text{decay}}(t) \equiv \langle \Upsilon_d(t)|\Upsilon_d(t)\rangle = 1 - P_{\text{surv}}(t)$, where $P_{\text{surv}}(t)$ is the so-called survival probability. That is

$$P_{\text{surv}}(t) = |\beta(t)|^2 = |\langle \Upsilon(0)|\Upsilon(t)\rangle|^2 . \tag{11}$$

In the second panel of Fig. 4, the survival probability is plotted in logarithmic scale: there is an oscillatory decay along time-evolution. Thus, this process is not alike the radioactive emission, since the exponential decay rule is hardly observed.

Indeed, the process can be interpreted as a superposition of the well-converged exponential decay and the fluctuation due to high-energy components. To confirm this, remembering that $P_{\text{surv}}(t) = 1 - P_{\text{decay}}(t)$, we decompose the decay probability into the low- and high-energy components by fixing the border of $E_T = 1.8$ MeV. That is,

$$
\begin{aligned}
P_{\text{decay}}(t) &= \sum_{E_M < E_T} |y_M(t)|^2 + \sum_{E_M \geq E_T} |y_M(t)|^2 \\
&\equiv P_{\text{decay}}(t; E < E_T) + P_{\text{decay}}(t; E \geq E_T) .
\end{aligned} \tag{12}
$$

Then, in Fig. 4, we plot the low-energy component of the survival probability: $P_{\text{surv}}(t; E < E_T) = 1 - P_{\text{decay}}(t; E < E_T)$. Consequently, it shows a smooth pattern and acquires an exponentially decaying form after $ct \geq 500$ fm. In this exponential decay, $P_{\text{surv}}(ct \geq 500 \text{ fm}; E < E_T) \simeq \exp(-t\Gamma/\hbar)$, where the decay-width is approximated as $\Gamma \simeq 0.41$ MeV in our calculation. Notice that this decay-width value is similar to the empirical values observed in several light one- and two-proton emitters [1, 2].

4. Summary

We have performed the time-dependent analysis of the emission process in the 1D three-body system. By monitoring the time-evolution from the initially confined state, we confirmed that two different types of emission are taking place: the earlier dinucleon emission, and the secondary separated emission. It is shown that, even for such a superposition of different processes, our time-dependent calculation can be a suitable tool to understand its multi-particle dynamics with an intuitive procedure. By analyzing the survival probability, we have also found that this process can be mainly interpreted as the exponential decay with $E < 1.8$ MeV plus the higher energy fluctuation. Further investigation of the origin of this fluctuation is an important future task. This investigation can lead to a deeper knowledge of the nuclear meta-stable systems, *e.g.* tetra neutron, whose measured decay-

width is considerably wide and hardly allows us to infer an exponential-decay behavior [4]. Our extension of the time-dependent method applied to these realistic 3D nuclear systems is in progress now.

REFERENCES

[1] L.V. Grigorenko *et al.*, *Phys. Lett. B* **677**, 30 (2009).

[2] M. Pfützner, M. Karny, L.V. Grigorenko, K. Riisager, *Rev. Mod. Phys.* **84**, 567 (2012).

[3] Y. Kondo *et al.*, *Phys. Rev. Lett.* **116**, 102503 (2016).

[4] K. Kisamori *et al.*, *Phys. Rev. Lett.* **116**, 052501 (2016).

[5] K. Fossez, J. Rotureau, N. Michel, M. Płoszajczak, *Phys. Rev. Lett.* **119**, 032501 (2017).

[6] E.E. Salpeter, *Astrophys. J.* **115**, 326 (1952).

[7] F. Hoyle, *Astrophys. J. Suppl. Ser.* **1**, 121 (1954).

[8] H. Suno, Y. Suzuki, P. Descouvemont, *Phys. Rev. C* **94**, 054607 (2016).

[9] R. Smith *et al.*, *Phys. Rev. Lett.* **119**, 132502 (2017).

[10] T. Myo *et al.*, *Prog. Part. Nucl. Phys.* **79**, 1 (2014).

[11] S.A. Gurvitz, G. Kalbermann, *Phys. Rev. Lett.* **59**, 262 (1987).

[12] S.A. Gurvitz, P.B. Semmes, W. Nazarewicz, T. Vertse, *Phys. Rev. A* **69**, 042705 (2004).

[13] T. Maruyama, T. Oishi, K. Hagino, H. Sagawa, *Phys. Rev. C* **86**, 044301 (2012).

[14] T. Oishi, K. Hagino, H. Sagawa, *Phys. Rev. C* **90**, 034303 (2014).

[15] L. Fortunato, T. Oishi, `arXiv:1701.04684 [nucl-th]` (under review).

[16] L.M. Delves, *Nucl. Phys.* **20**, 275 (1960).

[17] V. Aquilanti, A. Beddoni, A. Lombardo, R. Littlejohn, *Int. J. Quantum Chem.* **89**, 277 (2002).